Romanian Reports in Physics, Vol. 68, No. 3, P. 1115–1122, 2016

INVESTIGATION OF MULTILEVEL STRUCTURE OF LOW VISCOSITY SODIUM ALGINATE BY SMALL-ANGLE NEUTRON SCATTERING

C.R. BADITA[1,3], D. ARANGHEL[1,2], A. RADULESCU[4], E.M. ANITAS[1,5]

[1]"Horia Hulubei" National Institute for Nuclear Physics and Engineering, Reactorului 30, RO-077125, POB-MG6 Bucharest-Magurele, Romania, Email: daranghe@nipne.ro
[2]Extreme Light Intrastructure Nuclear Physics (ELI-NP), Reactorului 30, RO-077125, POB-MG6, Bucharest-Magurele, Romania
[3]University of Bucharest, Faculty of Physics, Atomiştilor 405, CP MG-11, RO – 077125, Bucharest-Magurele, Romania
[4]Forschungszentrum Jülich GmbH, Jülich Centre for Neutron Science, 85747 Garching, Germany
[5]Joint Institute for Nuclear Research, 141980 Dubna, Moscow region, Russian Federation

Received March 7, 2016

Abstract. The multilevel structure of low viscosity sodium alginate was studied by Small-Angle Neutron Scattering (SANS). Low viscosity sodium alginate is a water soluble biopolymer extracted from brown seaweed and is also used by many industries due their ability to create films, foams and fibers. Here we present the morphology of the low viscosity sodium alginate at various concentrations of low viscosity sodium alginate and calcium chloride as revealed by SANS technique in the q-interval 0.001 $Å^{-1} < q < 0.5$ $Å^{-1}$. To characterize the structural properties of the sodium alginate solutions the Beaucage model was applied.

Key words: low viscosity sodium alginate; fractal structures; small angle neutron scattering (SANS).

1. INTRODUCTION

In the past years the interest in using natural materials has increased, due to their biocompatibility and their lack of environment load upon disposal.

Sodium alginate is a natural polysaccharide product extracted from the cell wall of brown seaweed and is the sodium salt of alginic acid. Due to its viscosity, it is used as an emulsifier and a gelling agent in many industries. It is a linear copolymer with homopolymeric blocks of β-d-mannuronic acid (M) and α-l-guluronic acid (G) monomers, covalently linked together in different sequences or blocks. The monomers can appear in homopolymeric blocks of consecutive G-residues (G-blocks), consecutive M-residues (M-blocks) or alternating M and G-residues (MG-blocks) [1].

It is a water soluble biopolymer which in the presence of divalent cations, such as calcium, forms a three-dimensional network (gel), whose conformation is described by "egg box" model [2–4]. Although many studies have been performed, there are still unsolved some problems related to the mechanism of the gelation.

This paper presents our results concerning the morphology of low viscosity sodium alginate solutions at various concentrations and shows how their properties can be influenced by adding amounts of salt affecting the surface morphology. To characterize these solutions, the Small-Angle Neutron Scattering (SANS) method was applied. Experimental data were investigated by the multi-level Beaucage model [5]. The Beaucage model [6, 7] is often used to model SAS data in order to extract the radius of gyration and the Porod exponent for each level.

The obtained information from the SANS curves help to understand the distribution of the particles in the polymer matrix thereby enabling control over material properties [8].

2. MATERIALS AND METHODS

The following materials were used in our study: low viscosity sodium alginate samples, having the chemical formula $(C_6H_9O_7Na)_n$ and calcium chloride dihydrate 99% ($CaCl_2 \cdot 2H_2O$). These materials were purchased from "Alpha Aesar, A Johnson Mathey Company". Alginic acid sodium salt, low viscosity has the viscosity of 40–90 mPas (1% solution) and the pH of 5.0–7.5 (1% solution).

0.5%, 1.0%, 2.0% and 5.0 wt % by mass fraction of low viscosity sodium alginate were mixed in D_2O. To distinguish if the properties of sodium alginate can be influenced by adding amounts of salt, solutions of low viscosity sodium alginate were combined with 0.5% and 1.5 % calcium chloride. The samples were contained in quartz cuvettes of 1 mm and 2 mm path length.

The SANS experiments were carried out at Jülich Centre for Neutron Science at Garching (Germany), FRM II, research reactor Munich II. The experimental data were acquired using the KWS-2 diffractometer with sample-detector distances of 2, 4 and 8 m and wavelengths of 4.5 and 19 Å, respectively. The range of scattering vector was between 0.001 and 0.5 $Å^{-1}$. The measurements were done at 20 ºC. Scattering from samples was corrected taking into account the detector background and sensitivity, empty cell scattering, incoherent scattering, sample transmission and cell thickness. Solvent intensity was extracted from that of the sample [9].

Based on the polymer fractal model, the Beaucage model allows the usage of both the Guinier and the Porod laws, yielding a radius of gyration and a Porod exponent [10]. The multi-level Beaucage model [5, 7, 11–13] describes the scattering intensity for each succeeding structural level as a function of momentum transfer vector, $q = 4\pi / \lambda \cdot \sin(\theta / 2)$:

$$I(q) \approx \sum_{i=1}^{n} \left(G_i \exp\left(-\frac{q^2 R_{gi}^2}{3} \right) + B_i \exp\left(-\frac{q^2 R_{g(i+1)}^2}{3} \right) \left[\frac{\left(erf\left(\frac{kqR_{gi}}{sqrt(6)} \right) \right)^3}{q} \right]^{P_i} \right) + A, \quad (1)$$

where n is the number of structural levels observed, G_i are Guinier prefactors, B_i are prefactors specific to the type of power-law scattering, specified by the regime in which the exponent P_i falls, *k* is an empirical constant with a value close to 1.06 [7], *erf* is the error function and A is the background.

Each structural level i is described by four parameters G_i, B_i, R_{gi} and P_i [6], $i = 1$, refers to the largest size structure composed of small-scale structures of average size $R_{g(i+1)}$ [11]. The power-law prefactor is written for an arbitrary polymeric-mass fractal [5] as:

$$B_i = \left(\frac{G_i \cdot P_i}{R_{gi}^{P_i}} \right) \cdot \Gamma\left(\frac{P_i}{2} \right), \quad (2)$$

where Γ is gamma function.

The non-integer values of P_i implies a fractal analysis. If the power-law exponent $1 < P_i < 3$, the measured sample is a mass fractal, while if $3 < P_i < 4$ then the sample is a surface fractal. In the case of mass fractals, the fractal dimension $D_m = P_i$ and for surface fractals the fractal dimension $D_s = 6 - P_i$ [14, 15].

In the case of correlated particles, the scattering intensity is given by:

$$I(q) = AP(q)S(q), \quad (3)$$

where $AP(q)$ correspond to the scattered intensity for non-correlated domains and $S(q)$ is a structure factor which account for correlations of the domains [3]. A semi-empirical function for $S(q)$ which describes damped spherical correlations of colloidal particles can be written as [5]:

$$S(q) = \frac{1}{1 + \eta \cdot 3\frac{\sin(q\xi) - q\xi\cos(q\xi)}{(q\xi)^3}}, \quad (4)$$

where η describes the degree of correlations ($0 < \eta < 6$), $3\frac{\sin(q\xi) - q\xi\cos(q\xi)}{(q\xi)^3}$ is the "form factor" for spherical interactions correlated over a correlation length

ξ corresponding to the average distance between spherically correlated particles [10, 11].

The scattering intensity for weakly correlated particles $0 < \eta < 3$ becomes:

$$I(q) \approx \left[\sum_{i=1}^{n} \left(G_i \exp\left(-\frac{q^2 R_{gi}^2}{3} \right) + B_i \exp\left(-\frac{q^2 R_{g(i+1)}^2}{3} \right) \left[\frac{\left(erf\left(\frac{kqR_{gi}}{sqrt(6)} \right) \right)^3}{q} \right]^{P_i} \right) + A \right] \times \tag{5}$$

$$\times \frac{1}{1 + \eta \cdot 3 \frac{\sin(q\xi) - q\xi\cos(q\xi)}{(q\xi)^3}}.$$

Fitting the experimental data using equation (5), the fractal dimensions, the Guinier pre-factors G_i, the Porod exponents for the corresponding function P_i, radii of gyrations R_{gi}, the degree of correlation η, and correlation lengths ξ were obtained.

3. RESULTS AND DISCUSSIONS

SANS data information on the organization of the sodium alginate molecules over a length scale range $2\pi / q$ that extended from 12 to 6000 Å are shown in Fig. 1 on a double logarithmic scale from the different concentrations. The scattered intensity and the fitting parameters obtained from the SANS curves are dependent functions of low viscosity sodium alginate concentration. The solutions display a peak which is due both the periodic microphase separated morphology in the ordered phase and the correlation hole effect in the disordered phase [16]. Increasing the concentration of sodium alginate, the peak becomes broader and weaker, gradually disappearing.

For 0.5% and 1.0% low viscosity sodium alginate concentrations one observes that the scattering exponent absolute values are ranging between 3.52 and 3.27 (see Table 1). These values normally indicate scattering from fractally rough surfaces yielding D_s values of 2.48 and 2.73. The estimated "particle" sizes from Guinier regime is about 760 and 855 Å.

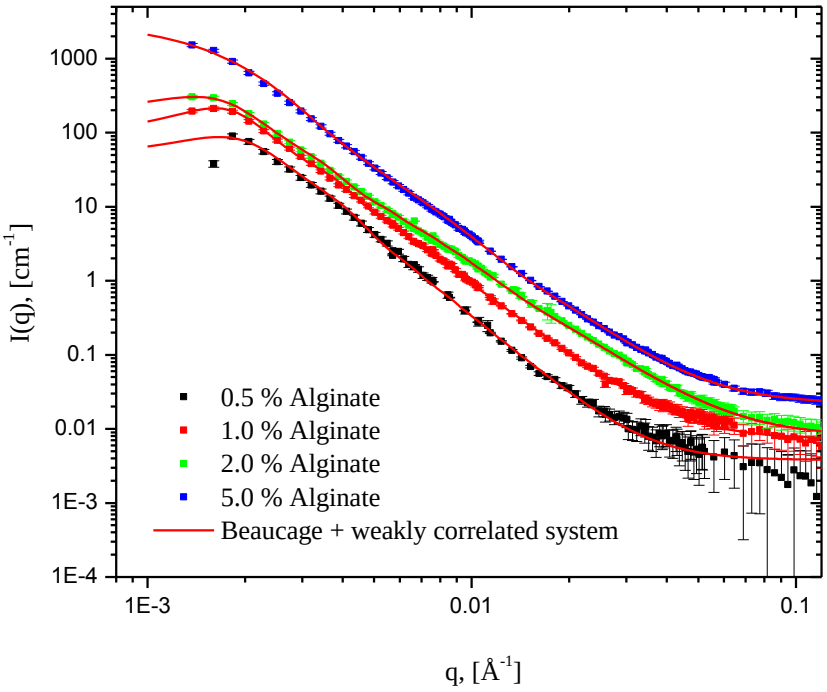

Fig. 1 – Fits of the SANS data for different concentrations of sodium alginate using equation (5).

For concentrations greater than or equal to 2.0% low viscosity sodium alginate concentration the scattering curves are characterized by two regions separated by a "knee" corresponding to the Guinier and Porod regimes yield approximate estimates of the size and the shape of the aggregates and of the primary particles, respectively. Therefore, to fit these data we chose the Beaucage model with two structural levels [17] which accounts the weak correlations of the domains [10]. The calculated structural parameters for these fits are given also in Table 1. At low q, these functions have a Porod exponent (P_1) between 3.06 and 3.10 corresponding to surface fractal dimensions (D_s) between 2.94 and 2.90. All values indicate that the scattering is given by fractal structures with rough surface [18]. At high q the Porod exponents have values of 2.74 and 2.98 that are specific to mass fractals. We can see that the correlation length ξ of weakly correlated particles grow with the concentration increase of the sodium alginate. Also, the peak shifts to lower q with increasing concentration, indicating an increase of the correlation length size ξ and a decrease of degree of correlation η, respectively.

Table 1

Fitting parameters obtained from the SANS data analysed using the empiric Beaucage model for different concentrations of alginates

Samples	G_1 **[cm^{-1}]**	P_1	R_{g1} **[Å]**	G_2 **[cm^{-1}]**	P_2	R_{g2} **[Å]**	η	ξ **[Å]**
0.5% Alginate	125	3.52	760	–	–	–	3.12	2800
1.0% Alginate	324	3.27	855	–	–	–	2.63	3189
2.0% Alginate	520	3.06	970	8.8	2.74	258	2.08	3302
5.0% Alginate	3183	3.10	1149	11.5	2.98	214	1.20	3558

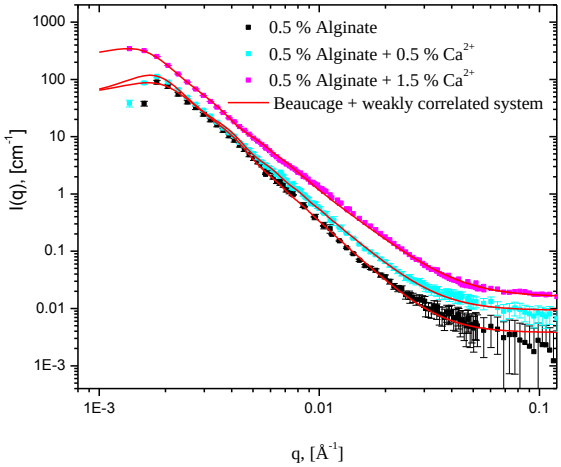

(a)

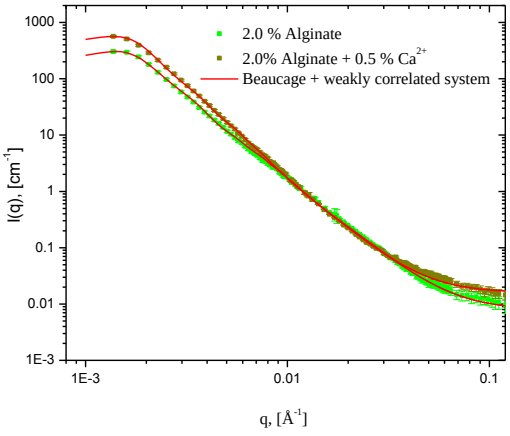

(b)

Fig. 2 – Fits of the SANS data for two concentrations (0.5 % and 2.0 %) of sodium alginate mixed with different concentrations of calcium chloride using equation (5).

As well, the mixtures of the alginate with Ca^{2+} were modelled using eq. (5) and are shown in Fig. 2. Porod exponents at the low q region (P_1) are typical for the rough surface fractals (see Table 2) and these give a specific surface fractal dimension D_s of 2.75, 2.82 and 2.80. Adding Ca^{2+} increases the size of the aggregates and shorten the size of the primary particles [19].

From Table 2 we can see the primary particles are represented by mass fractals which tend to have a globular three-dimensional shape and these agglomerates in aggregates represented by fractally rough surfaces [20–24].

Table 2

Fitting parameters obtained from the SANS data analysed using the empiric Beaucage model for mixed sodium alginate solutions with calcium

Samples	G_1 [cm^{-1}]	P_1	R_{g1} [Å]	G_2 [cm^{-1}]	P_2	R_{g2} [Å]	η	ξ [Å]
0.5% Alginate + 0.5%Ca^2	170	3.25	825	–	–	–	2.63	2900
0.5%Alginate + 1.5%Ca^2	618	3.18	1036	8.0	2.90	272	2.06	3388
2.0%Alginate + 0.5%Ca^2	917	3.20	967	8.0	2.96	234	1.77	3528

The values obtained from Beaucage model (Tables 1 and 2) validate the assumption that the addition of salt induces the collapse and it determines the formation of the secondary structure above a certain concentration, which we call it critical concentration.

4. CONCLUSIONS

To investigate the morphology of low viscosity sodium alginate at various concentrations, the hierarchical Beaucage model was applied. Because at low q the data presents an apparent peak, they were modelled considering the structure factor which accounts the weak correlations of the domains. The results indicate that the sodium alginate in the presence/absence of Ca^{2+} is characterized by spherical morphology at the scattering "particle" sizes between 214 and 272 Å for primary particles and sizes between 760 and 1149 Å for aggregates. The aggregate structures are seen in the low-q region ($i=1$) and are made up from primary particles.

Adding salt accelerate the gelation process, induce the collapse and shorten sodium alginate chains due to alginate stiffening. The critical concentration for secondary structure formation is 2.0% of the substance dissolved (low viscosity

sodium alginate with/without Ca^{2+}). At this value a transition occurs from a rough surface fractal-like structure to a mass fractal structure.

Acknowledgements. This material is partly based upon work supported by the European Commission under the 7th Framework Programme through the Key Action: Strengthening the European Research Area, Research Infrastructures, Contract n°: 26507 (NMI3) and the international cooperation projects JINR, Russia – IFIN-HH, Romania.

REFERENCES

1. Bernd H. A. Rehm, *Microbial Production of Biopolymers and Polymer Precursors: Applications and Perspectives*, Caister Academic Press, 2009.
2. K. I. Draget, O. Smidsrød, G. Skjåk-Bræk, *Alginates from Algae from Polysaccharides and Polyamides in the Food Industry*, A. Steinbuchel, S. K.Rhee, Wiley-Blackwell, London, 2005.
3. P. Sikorski, F. Mo, G. Skjåk-Bræk and B. T. Stokke, Biomacromolecules **8**, *7*, 2098–2103 (2007).
4. I. Braccini and S. Pérez, Biomacromolecules **2**, 1089–1096 (2001).
5. G. Beaucage, D. W Schaefer, J Non-Cryst. Solids **172**–**174**, 797–805 (1994).
6. G. Beaucage, J. Appl. Co, st. **29**, 134–146 (1996).
7. Boualem Hammouda , J. Appl. Cryst. **43**, 716–719 (2010).
8. E. M. Anitas, M. Balasoiu, I. Bica, V. A. Osipov, A. I. Kuklin, OAM-RC **3**, *6*, 621–624 (2009).
9. A. Radulescu, V. Pipich, H. Frielinghaus and M.-S. Appavou, J. Phys.: Conf. Ser. **351**, 012026 (2012).
10. Boualem Hammouda , J. Appl. Cryst. **43**, 1474–1478 (2010).
11. G. Beaucage, Polymer Science: A Comprehensive Reference **2**, 399–409 (2012).
12. V. A. Hackley, P. K. Stoimenov, D. L. Ho, L. P. Sung and K. J. Klabunde, J. Appl. Cryst. **38**, 619–631 (2005).
13. E. O. Jonah, D. T. Britton, P. Beaucage, D. K. Rai, G. Beaucage, B. Magunje, J. Ilavsky, M. R. Scriba, M. Härting, J. Nanopart. Res. **14**, 1249 (2012).
14. E. M. Anitas, I. Bica, R. V. Erhan, M. Bunoiu, A. I. Kuklin, Rom. J. Phys. **60**, *5–6*, 653–657 (2015).
15. C. Ionescu, C. Savii, M. Balasoiu, M. Popovici, C. Enache, A. Kuklin, A. Islamov, Y. Kovalev and L. Almásy, APTEFF **35**, 1–280, 95–101 (2004).
16. http://www.ncnr.nist.gov/staff/hammouda/the_SANS_toolbox.pdf
17. J. Hyeon-Lee, G. Beaucage, S. E. Pratsinis and S. Vemury, Langmuir **14**, 5751–5756 (1998).
18. A. Muñoz, J. Martínez, M.A. Monge, B. Savoini, R. Pareja, A. Radulescu, Int. Journal of Refractory Metals and Hard Materials **33**, 6–9 (2012).
19. L. L. Hyland, M. B. Taraban, B. Hammouda, Y. B. Yu, Biopolymers **95**, *12*, 840–851 (2011).
20. G. Beaucage, J. Appl. Cryst. **28**, 717–728 (1995).
21. G. J. Schneider, D. Göritz, J. Chem. Phys. **132**, 154903 (2010).
22. G. Beaucage, Biophys. J. **95**, *2*, 503–509 (2008).
23. D.W. Schaefer, T. Rieker, M. Agamalian, J.S. Lin, D. Fischer, S. Sukumaran, C. Chen, G. Beaucage, C. Herd and J. Ivie, J. Appl. Cryst. **33**, 587–591 (2000).
24. P. Sikorski, F. Mo, G. Skjåk-Bræk and B. T. Stokke, Biomacromolecules **8**, *7*, 2098–2103 (2007).